

Amplitude, phase, and topological fluctuations shaping the complex phase diagram of two-dimensional superconductors

Koichiro Furutani,^{1, 2,*} Giovanni Midei,³ Andrea Perali,⁴ and Luca Salasnich^{5, 6, 7}

¹*Department of Applied Physics, Nagoya University, Nagoya 464-8603, Japan*

²*Institute for Advanced Research, Nagoya University, Nagoya 464-8601, Japan*

³*School of Science and Technology, Physics Division, Università di Camerino,*

Via Madonna delle Carceri 9, 62032 Camerino, Italy

⁴*School of Pharmacy, Physics Unit, Università di Camerino,*

Via Madonna delle Carceri 9, 62032 Camerino, Italy

⁵*Dipartimento di Fisica e Astronomia 'Galileo Galilei' and QTech Center,*

Università di Padova, via Marzolo 8, 35131 Padova, Italy

⁶*Istituto Nazionale di Fisica Nucleare, Sezione di Padova, via Marzolo 8, 35131 Padova, Italy*

⁷*Istituto Nazionale di Ottica del Consiglio Nazionale delle Ricerche, via Carrara 2, 50019 Sesto Fiorentino, Italy*

(Dated: July 16, 2024)

We study the amplitude and phase fluctuations of the Ginzburg-Landau quasi-order parameter for superconductors in two spatial dimensions. Starting from the mean-field critical temperature T_{c0} , we calculate the beyond-mean-field critical temperature T_c by including thermal fluctuations of the quasi-order parameter within the Gaussian level. Moreover, from our beyond-mean field results, we derive the Berezinskii-Kosterlitz-Thouless critical temperature T_{BKT} , which takes into account topological vortex-antivortex excitations in the phase fluctuations as well as the amplitude fluctuations, to obtain the shifts of transition temperatures. We elucidate how the Gaussian thermal fluctuations and phase fluctuations associated with vortex excitations affect thermodynamic properties by determining the H - T phase diagram for a type-II superconductor and computing the critical behaviors of the heat capacity, which are experimentally accessible, allowing the characterization of the cascade of different kinds of fluctuations in 2D superconductors.

I. INTRODUCTION

Phase transitions in low-dimensional systems are central targets in modern physics and critical fluctuations play a crucial role in shaping their complex phase diagram, while featuring several anomalous properties detectable in experiments. The Ginzburg-Landau theory describes the behavior of an order parameter in a superconductor near the superconducting transition under spontaneous symmetry breaking, which captures a broad range of phase transitions including second-order phase transitions of superconductors or superfluids [1], multi-band superconductors [2–5], and twisted bilayer graphene [6]. Two-dimensional superconductors or superfluids, however, undergo a topological phase transition without spontaneous symmetry breaking, which is referred to as the Berezinskii-Kosterlitz-Thouless (BKT) transition [7, 8]. BKT transitions were first observed in a thin ^4He film [9]. Later, it was experimentally observed also in thin and disordered superconducting films [10–13] and a ^{39}K atomic gas [14] through the measurement of sound velocities [15, 16]. Phase fluctuations associated with the vortex excitations suppressing the superconducting transition temperature play a key role in the BKT transition. As exemplified by BKT physics, identifying what kind of fluctuations govern the microscopic behavior of a material is imperative to reveal the phase diagram. For instance, it has been investigated through

measurements of thermodynamic quantities such as the heat capacity [17–20] and the resistivity or the I - V characteristics [12]. The recent experiment in Ref. [20] reports spectroscopic and thermodynamic investigations of the iron-based superconductor $\text{FeSe}_{1-x}\text{S}_x$ throughout the Bardeen-Cooper-Schrieffer-Bose-Einstein-condensate (BCS-BEC) crossover [21], suggesting the dominant role of Gaussian thermal fluctuations in the vicinity of criticality.

In two-dimensional materials, in particular, the occurrence of off-diagonal long-range order (ODLRO) is ruled out at finite temperatures [22, 23], and the BKT transition is an infinite-order phase transition toward a quasi-long range ordered state [24], which hinders singularities of thermodynamic quantities in the vicinity of the transition point making the role of respective fluctuations difficult to establish across the BKT transition. These specific features of two-dimensional materials have motivated several attempts to clarify the dominant fluctuations and their evolution from the normal to the superconducting state both theoretically and experimentally. In the normal phase of cuprate superconductors in the underdoped regime, where the electronic behavior is practically two-dimensional, phase fluctuations are predicted to mainly contribute to the quasiparticle spectra [25]. The measurement of the Nernst coefficient supports that vortex excitations survive even well above the critical temperature, but quite below the pseudogap temperature; the doping dependence of the vortex excitations onset temperature shows the same dome-like behavior of the critical temperature [26]. The specific heat of cuprates

* koichiro.furutani@phd.unipd.it

is also affected by the pseudogap and exhibits similar peaked behavior as in FeSe [27]. Therefore, in two-dimensional strongly coupled superconductors, the superconducting transition is approached from the normal state through a weak-pseudogap phase at high temperature, where only amplitude fluctuations (Gaussian-like) are present, and then through a strong-pseudogap phase close to critical temperature, where also phase fluctuations are important and add their effects to the amplitude fluctuations, leading to well-formed pseudogap features and long-lived Cooper pairs (a quasi-condensate configuration). In a two-dimensional Fermi atomic gas above the superfluid transition temperature, a T -matrix analysis revealed that pseudogap grows with strong pairing fluctuations across the BCS-BEC crossover [28], which is in fair agreement with the experimental measurements of photoemission spectra with ^{40}K atoms [29, 30]. Theoretical works also predict the nonmonotonic behavior of the BKT transition temperature in terms of the pairing interaction strength [31, 32] and the upper bound [33] across the BCS-BEC crossover. On the other hand, in the context of ultracold atoms, experimental or theoretical investigations of the cooperative interplay between phase and amplitude fluctuations in determining strong pseudogap features are lacking, also considering that T -matrix approaches in two dimensions close to the critical temperature are ill-defined. The above discussion motivates us to investigate the cascade of fluctuations in two-dimensional superconductors exploring a wide temperature range across the critical temperature to disentangle the effect on the system properties of each type of fluctuation.

In this work, we consider two-dimensional superconductors to analyze the effects of both the Gaussian thermal fluctuations and topological phase fluctuations, which result in the BKT transition within the Ginzburg-Landau theory. We examine the fluctuations of different natures characterizing the phase diagram of the system and discuss their roles in the renormalization of the superconducting critical temperature. In Sec. III, we start from the Ginzburg-Landau free energy and show the mean-field analysis. In Sec. IV, we include thermal fluctuations at the Gaussian level, which lowers the critical temperature from the mean-field one. In Sec. V, we further incorporate the vortex excitations responsible for the BKT transition by solving the Nelson-Kosterlitz (NK) renormalization group equations. We discuss the roles of both the Gaussian thermal fluctuations and phase fluctuations associated with vortex excitations, and obtain a formula for the shift of critical temperatures. To this end, we employ a semi-analytic relation between the bare and the renormalized phase stiffness. Finally, we determine and discuss the H - T phase diagram of a typical type-II superconductor in Sec. VI and the critical behavior of the heat capacity in Sec. VII, which highlights the roles of fluctuations. In particular, the phase fluctuations associated with vortex excitations turn out to drastically change the critical behavior of the heat ca-

pacity. Our results suggest that the measurement of the heat capacity in the vicinity of critical temperature can be utilized to verify what types of fluctuations govern a two-dimensional superconducting material. Section VIII summarizes our results. Details of numerical and analytic computations are reported in Appendices A, B, and C.

II. HOHENBERG-MERMIN-WAGNER'S THEOREM AND BKT TRANSITION

Before moving on to our analysis, we review quasi-long-range order (qLRO) in two-dimensional superconductivity and briefly summarize how to investigate the effects of amplitude fluctuations in two-dimensional superconductors subject to the BKT transition.

Hohenberg-Mermin-Wagner's theorem rules out spontaneous symmetry breaking at finite temperatures in an infinite-size system hosting short-range interaction and a continuous symmetry with spatial dimensions lower than three [22, 23]. It prohibits the occurrence of ODLRO at finite temperatures in two dimensions. With a superconducting order parameter ψ , it states the vanishing ensemble average $\langle \psi \rangle = 0$. This originates from enhanced infrared fluctuations in lower dimensions that break the ordered state in an infinite-size system. However, Berezinskii, Kosterlitz, and Thouless pointed out that dissipationless flow can occur in two dimensions by the formation of vortex-antivortex pairs at low temperatures even though the ODLRO is absent [7, 8]. As the temperature rises, the dissociation of neutral vortex-antivortex pairs occurs at a transition temperature and then the superconductivity is broken, which is the mechanism of the BKT transition. Then, the vortex fluctuations results in $\langle |\psi| \rangle \neq 0$ in the low-temperature phase even though $\langle \psi \rangle = 0$ [34]. We may call ψ the *quasi*-order parameter. The square of the ensemble average of the quasi-order parameter *modulus* can be indeed interpreted as the superfluid density. A salient feature of the BKT superconductor is the qLRO in the low-temperature phase described by the power-law decay of the single-body density matrix $\langle \psi(\mathbf{r})\psi(\mathbf{r}') \rangle \propto |\mathbf{r} - \mathbf{r}'|^{-\eta}$. The algebraic exponent η is related to the superfluid density and is a good indicator to verify the BKT transition.

There are several attempts to investigate the effects of amplitude fluctuations on the two-dimensional superconductors. One of the major approaches is the T -matrix analysis. The T -matrix analysis is, however, ill-defined due to the infrared divergence in two dimensions as dictated by Hohenberg-Mermin-Wagner's theorem. This problem can be solved by exploiting an infrared cutoff k_0 to keep the infrared divergence under control [28]. In this way, in Ref. [28], a successful comparison between theory and experiments for a 2D trapped Fermi system has been reported in the intermediate temperature range between the low-temperature region approaching the critical temperature from above and the high-

temperature region where the T -matrix describes a semi-classical system of attractive fermions. Once fluctuations are taken into account in this manner, superconducting fluctuations can be quantitatively evaluated by the T -matrix approach or the Ginzburg-Landau approach, which yields almost the same results. This treatment is also supported by experimental reports of the BCS-Bose-Einstein-quasi-condensation (BEqC) crossover phenomena including pseudogap formation and pair-size shrinking in 2D superconductors of Li_xZrNCl [12], which are similar to 3D cases. It is because the phenomenology is local in character and connected with a short-range scale common with 3D cases except in the vicinity of the BKT transition. In this paper, we investigate effects of fluctuations on the BKT transition by following this strategy.

III. GINZBURG-LANDAU FUNCTIONAL

Close to the critical temperature the free energy of a single-band superconducting material can be written as

$$F = F_n + F_s, \quad (1)$$

where F_n is the contribution due to the normal component and F_s is the contribution due to the emergence of a superconducting quasi-order parameter $\psi(\mathbf{r})$ below the critical temperature. Within the Ginzburg-Landau approach [1], for a two-dimensional system of area L^2 , the super component F_s is given by

$$F_s = \int_{L^2} d^2 \mathbf{r} \left\{ a(T) |\psi(\mathbf{r})|^2 + \frac{b}{2} |\psi(\mathbf{r})|^4 + \gamma |\nabla \psi(\mathbf{r})|^2 \right\}, \quad (2)$$

where

$$a(T) = \alpha k_{\text{B}} (T - T_{\text{c}0}) \quad (3)$$

is a parameter which depends on the temperature T and becomes zero at the mean-field (MF) critical temperature T_{c0} , while $b > 0$ and $\gamma > 0$ are temperature-independent parameters with k_B being the Boltzmann constant. The energy functional (2) and the values of the parameters α , b and γ can be deduced from the microscopic BCS theory as [35, 36]

$$\alpha = \frac{4\pi^2}{7\zeta(3)} \frac{T_{c0}}{T_F}, \quad b = \frac{7\zeta(3)}{8\pi^2} \frac{\alpha^2}{\nu}, \quad \gamma = \frac{\hbar^2}{4m}, \quad (4)$$

with T_F being the Fermi temperature, m being the electronic mass, $\nu = m/\pi\hbar^2$ being the density of states for two-dimensional electrons having a parabolic energy dispersion, and $\zeta(x)$ being the zeta function.

The partition function \mathcal{Z} of the system is given by

$$\mathcal{Z} \equiv e^{-\beta F_n} \mathcal{Z}_n \quad (5)$$

where

$$\mathcal{Z}_s = \int \mathcal{D}[\psi(\mathbf{r})] e^{-\beta F_s[\psi(\mathbf{r})]} \quad (6)$$

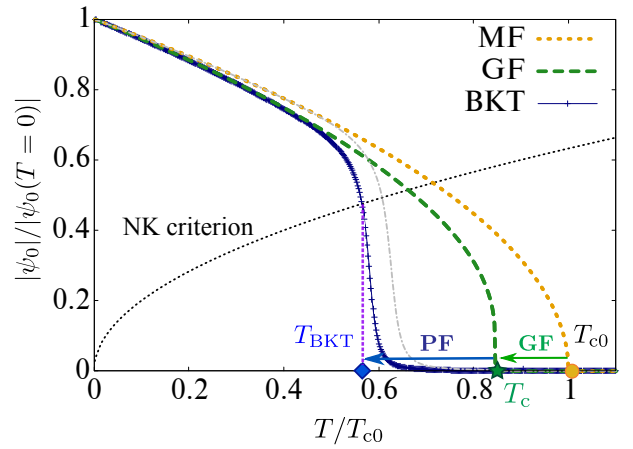


FIG. 1. Modulus of the quasi-order parameters as a function of the temperature T . The quasi-order parameter ψ_0 is obtained at the MF level with Eq. (11) (dotted curve), $\psi_0^{(\text{GF})}$ is derived including the Gaussian fluctuations (GF) in Eq. (19) with Eq. (40) (dashed curve), and $\psi_R^{(\text{BKT})} = \sqrt{J_R(T)/2\gamma}$ is determined by Eqs. (58) and (59) including the phase fluctuations (PF) associated with vortex excitations responsible for the BKT transition under $l_{\max} = \ln(\pi/\xi k_0)$ (solid curve). We set $\text{Gi} = 0.1$. The gray dotted-dashed curve represents the order parameter obtained by Eqs. (58) and (59) under the MF bare values without the Gaussian fluctuations. These quasi-order parameters vanish at different critical temperatures: T_{c0} at the MF level, T_c at the GF level without vortices, and T_{BKT} including the vortex excitations. The thin dotted black curve represents $k_B T = \pi\gamma|\psi_0|^2$, which stands for the NK criterion. It intersects with the quasi-order parameter at T_{BKT} (vertical violet dashed line).

is the partition function of the superconducting component with $\beta = 1/k_B T$. The thermal average of an observable \mathcal{O} that is a functional of $\psi(\mathbf{r})$ reads

$$\langle \mathcal{O} \rangle = \frac{1}{Z_s} \int \mathcal{D}[\psi(\mathbf{r})] \mathcal{O}[\psi(\mathbf{r})] e^{-\beta F_s[\psi(\mathbf{r})]} . \quad (7)$$

By assuming a real and uniform quasi-order parameter, i.e.

$$\psi(\mathbf{r}) = \psi_0 , \quad (8)$$

the energy functional (2) with Eqs. (3) and (8) becomes

$$\frac{F_{\text{so}}[\psi_0]}{J^2} = a(T) \psi_0^2 + \frac{b}{2} \psi_0^4. \quad (9)$$

Minimizing F_{s0} with respect to ψ_0 , one immediately finds

$$a(T) \psi_0 + b \psi_0^3 \equiv 0 , \quad (10)$$

and consequently

$$\psi_0 = \begin{cases} 0 & \text{for } T \geq T_{c0}, \\ \sqrt{-\frac{a(T)}{b}} & \text{for } T < T_{c0}. \end{cases} \quad (11)$$

The uniform quasi-order parameter ψ_0 becomes different from zero only below the MF critical temperature T_{c0} , where, by definition, T_{c0} is such that

$$a(T_{c0}) = 0. \quad (12)$$

The temperature dependence of the mean-field quasi-order parameter (11) is shown in Fig. 1.

IV. GAUSSIAN FLUCTUATIONS OF THE QUASI-ORDER PARAMETER

Extremizing the functional (2) with respect to $\psi^*(\mathbf{r})$ one gets the Euler-Lagrange equation

$$a(T) \psi + b |\psi|^2 \psi - \gamma \nabla^2 \psi = 0. \quad (13)$$

We write the space-dependent quasi-order parameter $\psi(\mathbf{r})$ as

$$\begin{aligned} \psi(\mathbf{r}) &= [\psi_0^{(\text{GF})} + \sigma(\mathbf{r})] e^{i\theta_0(\mathbf{r})} \\ &\simeq \psi_0^{(\text{GF})} + \eta(\mathbf{r}), \end{aligned} \quad (14)$$

where $\eta(\mathbf{r}) = \sigma(\mathbf{r}) + i\theta_0(\mathbf{r})\psi_0^{(\text{GF})}$ represents fluctuations of both amplitude and phase to the first order with respect to the real and uniform configuration $\psi_0^{(\text{GF})}$ with the condition

$$\langle \eta \rangle = \langle \eta^* \rangle = 0, \quad (15)$$

where $\langle \cdot \rangle$ is the thermal average. Inserting Eq. (14) into Eq. (13), we find

$$\begin{aligned} a(T) \psi_0^{(\text{GF})} &+ b (\psi_0^{(\text{GF})})^3 + a(T) \eta + 2b (\psi_0^{(\text{GF})})^2 \eta \\ &+ b (\psi_0^{(\text{GF})})^2 \eta^* + 2b \psi_0^{(\text{GF})} |\eta|^2 \\ &+ b \psi_0^{(\text{GF})} \eta^2 + b |\eta|^2 \eta - \gamma \nabla^2 \eta = 0, \end{aligned} \quad (16)$$

and after thermal averaging we obtain

$$[a(T) + 2b \langle |\eta|^2 \rangle + b \langle \eta^2 \rangle] \psi_0^{(\text{GF})} + b (\psi_0^{(\text{GF})})^3 + b \langle |\eta|^2 \eta \rangle = 0. \quad (17)$$

Clearly, only by removing all thermal averages, one recover Eq. (10) and find that $\psi_0^{(\text{GF})}$ is equal to ψ_0 and given by Eq. (11). In the framework of the Gross-Pitaevskii equation, this is called the Bogoliubov approximation [37].

We take into account thermal fluctuations of the quasi-order parameter keeping $\langle |\eta|^2 \rangle$ but neglecting the anomalous averages $\langle \eta^2 \rangle$ and $\langle |\eta|^2 \eta \rangle$. This is the so-called Popov approximation [37]. In this way, we get

$$[a(T) + 2b \langle |\eta|^2 \rangle] \psi_0^{(\text{GF})} + b (\psi_0^{(\text{GF})})^3 = 0, \quad (18)$$

and consequently

$$\psi_0^{(\text{GF})} = \begin{cases} 0 & \text{for } T \geq T_c, \\ \sqrt{-\frac{a(T) + 2b \langle |\eta|^2 \rangle}{b}} & \text{for } T < T_c. \end{cases} \quad (19)$$

In this case, the uniform quasi-order parameter $\psi_0^{(\text{GF})}$ becomes different from zero only below the beyond-MF critical temperature T_c determined by

$$a(T_c) + 2b \langle |\eta|^2 \rangle_c = 0, \quad (20)$$

with $\langle |\eta|^2 \rangle_c \equiv \langle |\eta|^2 \rangle_{T \rightarrow T_c^+}$. The free energy generating Eq. (18) including the Gaussian thermal fluctuations is given by

$$\frac{F_{\eta}^{(\text{GF})}}{L^2} = \left[a(T) + 2b \langle |\eta|^2 \rangle \right] (\psi_0^{(\text{GF})})^2 + \frac{b}{2} (\psi_0^{(\text{GF})})^4. \quad (21)$$

It is important to stress that, to treat self-consistently the fluctuating field $\eta(\mathbf{r})$, the Popov approximation requires $|\eta|^2 \eta \simeq 2 \langle |\eta|^2 \rangle \eta$, $|\eta|^2 \simeq \langle |\eta|^2 \rangle$, and $\eta^2 \simeq 0$ in Eq. (16) [37], which becomes

$$a(T) \eta + 2b (\psi_0^{(\text{GF})})^2 \eta + 2b \langle |\eta|^2 \rangle \eta + b (\psi_0^{(\text{GF})})^2 \eta^* - \gamma \nabla^2 \eta = 0, \quad (22)$$

taking into account Eq. (18). Notice that the Popov approximation gives a gapless spectrum, as required by the Goldstone theorem [37].

Let us work with $T \geq T_c$ where $\psi_0^{(\text{GF})} = 0$. Then, Eq. (22) reduces to

$$a(T) \eta + 2b \langle |\eta|^2 \rangle \eta - \gamma \nabla^2 \eta = 0, \quad (23)$$

which is the Euler-Lagrange equation of the Gaussian energy functional

$$\begin{aligned} F_{\eta}^{\text{Popov}}(T \geq T_c) &= \int_{L^2} d^2 \mathbf{r} \left[(a(T) |\eta(\mathbf{r})|^2 + 2b \langle |\eta|^2 \rangle) |\eta(\mathbf{r})|^2 \right. \\ &\quad \left. + \gamma |\nabla \eta(\mathbf{r})|^2 \right]. \end{aligned} \quad (24)$$

Expanding the field $\eta(\mathbf{r})$ in a plane-wave basis, i.e.

$$\eta(\mathbf{r}) = \frac{1}{L} \sum_{\mathbf{k}} \tilde{\eta}_{\mathbf{k}} e^{i\mathbf{k} \cdot \mathbf{r}}, \quad (25)$$

it is straightforward to find

$$F_{\eta}^{\text{Popov}}(T \geq T_c) = \sum_{\mathbf{k}} [a(T) + 2b \langle |\eta|^2 \rangle + \gamma k^2] |\tilde{\eta}_{\mathbf{k}}|^2. \quad (26)$$

The partition function \mathcal{Z} of the system is then given by

$$\begin{aligned} \mathcal{Z} &= e^{-\beta F_{\eta}^{\text{Popov}}} \int \mathcal{D}[\eta(\mathbf{r})] e^{-\beta F_{\eta}^{\text{Popov}}[\eta(\mathbf{r})]} \\ &= e^{-\beta F_{\eta}^{\text{Popov}} - \beta F_{\text{fl}}^+}, \end{aligned} \quad (27)$$

where

$$\begin{aligned} F_{\text{fl}}^+ &= -\frac{1}{\beta} \ln \int \mathcal{D}[\eta(\mathbf{r})] e^{-\beta F_{\eta}^{\text{Popov}}[\eta(\mathbf{r})]} \\ &= -\frac{1}{\beta} \sum_{\mathbf{k}} \ln \left(\frac{\pi k_B T}{a(T) + 2b \langle |\eta|^2 \rangle + \gamma k^2} \right), \end{aligned} \quad (28)$$

represents the contribution of the thermal fluctuations to the free energy above T_c . The thermal average

$$\langle |\eta|^2 \rangle = \frac{1}{Z_\eta} \int \mathcal{D}[\eta(\mathbf{r})] |\eta(\mathbf{r})|^2 e^{-\beta F_\eta^{\text{Popov}}[\eta(\mathbf{r})]} \quad (29)$$

reads

$$\langle |\eta|^2 \rangle = \frac{1}{\beta L^2} \sum_{\mathbf{k}} \frac{1}{a(T) + 2b\langle |\eta|^2 \rangle + \gamma k^2}, \quad (30)$$

with $Z_\eta \equiv \int \mathcal{D}[\eta(\mathbf{r})] \exp[-\beta F_\eta^{\text{Popov}}[\eta(\mathbf{r})]]$. At $T \rightarrow T_c+$, where Eq. (20) holds, we get

$$\langle |\eta|^2 \rangle_c = \frac{1}{L^2} \sum_{\mathbf{k}} \frac{k_B T_c}{\gamma k^2}. \quad (31)$$

In the continuum of momenta \mathbf{k} , where $\sum_{\mathbf{k}} = L^2 \int d^2 \mathbf{k} / (2\pi)^2$, we assume that some physical cutoff constrains the values of k [34]. Under this assumption, we find

$$\langle |\eta|^2 \rangle_c = \frac{k_B T_c}{2\pi\gamma} \ln \left(\frac{\Lambda}{k_0} \right), \quad (32)$$

where k_0 is an infrared cutoff and Λ an ultraviolet cutoff. Then, Eq. (20) gives

$$\frac{T_{c0} - T_c}{T_c} = 4 \text{Gi} \ln \left(\frac{\Lambda}{k_0} \right) \quad (33)$$

with

$$\text{Gi} = \frac{b}{4\pi\alpha\gamma} \quad (34)$$

the Ginzburg-Levanyuk number. With Eqs. (4), Eq. (34) reduces to $\text{Gi} = \pi T_{c0} / 2T_F$. According to Larkin and Varlamov [34], one has

$$\Lambda = \frac{1}{2\xi}, \quad k_0 = \frac{\sqrt{\text{Gi}}}{\xi} \quad (35)$$

with $\xi = (\gamma/\alpha k_B T_c)^{1/2}$ the coherence length. It follows that $\Lambda/k_0 = 1/(4\text{Gi})^{1/2}$ and consequently

$$\frac{T_{c0} - T_c}{T_c} = 2 \text{Gi} \ln \left(\frac{1}{4\text{Gi}} \right). \quad (36)$$

The shift in Eq. (36) coincides with Eq. (2.120) in Ref. [34] obtained via renormalization group analysis of the Ginzburg-Landau coefficients, which justifies the introduction of the infrared momentum cutoff k_0 . Interestingly, our choice of the infrared cutoff can be written as $k_0 = (4\text{Gi})^{1/2} \Lambda$ in such a way as to make clear its behavior approaching the weak-coupling regime. When the ultraviolet cutoff Λ is fixed and Gi goes to zero in the large density regime, k_0 scales toward zero, enhancing the region of validity of our approach. For very small Gi , the mean-field and the beyond mean-field Gaussian fluctuations physics will survive also very close to the phase

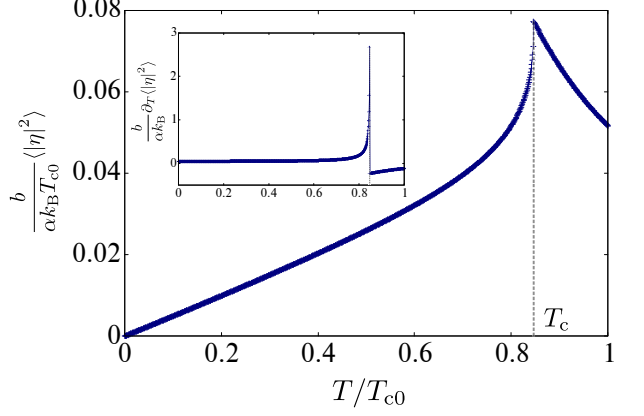


FIG. 2. Magnitude of the correction to the quasi-order parameter by the Gaussian fluctuations $\langle |\eta|^2 \rangle$ calculated from Eq. (40) below T_c and Eq. (30) above T_c with $\text{Gi} = 0.1$. The inset shows the temperature derivative $\partial_T \langle |\eta|^2 \rangle(T)$.

transition. This justifies our choice of k_0 , having the expected behavior when the weak-coupling BCS regime is approached by tuning the density (see the discussion reported in Ref. [28]). Note that this result takes into account both amplitude and phase fluctuations of the quasi-order parameter at the Gaussian level. See also Refs. [34, 39, 40]. However, Eq. (36) does not include the effects of the topological defects (quantized vortices and anti-vortices).

A. Gaussian fluctuations below T_c

To compute Eq. (19), we examine the Gaussian fluctuations (GF) below T_c . Instead of Eq. (23), $\langle |\eta|^2 \rangle$ is determined by Eq. (22). Then, Eq. (22) reads

$$\frac{\delta F_\eta^{\text{Popov}}}{\delta \eta^*} = 0, \quad (37)$$

with

$$\begin{aligned} F_\eta^{\text{Popov}} &\equiv \int d^2 \mathbf{r} \left[\left[a(T) + 2b(\psi_0^{\text{GF}})^2 \right] |\eta(\mathbf{r})|^2 \right. \\ &\quad \left. + 2b\langle |\eta|^2 \rangle |\eta(\mathbf{r})|^2 + \frac{b}{2} (\psi_0^{\text{GF}})^2 [\eta(\mathbf{r})^2 + \eta^*(\mathbf{r})^2] \right. \\ &\quad \left. + \gamma |\nabla \eta(\mathbf{r})|^2 \right] \\ &= \sum_{\mathbf{k}} \left[\left(a(T) + 2b\langle |\eta|^2 \rangle + 3b(\psi_0^{\text{GF}})^2 + \gamma k^2 \right) \tilde{\eta}'_{\mathbf{k}}^2 \right. \\ &\quad \left. + \left(a(T) + 2b\langle |\eta|^2 \rangle + b(\psi_0^{\text{GF}})^2 + \gamma k^2 \right) \tilde{\eta}''_{\mathbf{k}}^2 \right], \end{aligned} \quad (38)$$

where $\tilde{\eta}'_{\mathbf{k}}$ and $\tilde{\eta}''_{\mathbf{k}}$ are the real part and imaginary part, respectively, of $\tilde{\eta}_{\mathbf{k}} = \tilde{\eta}'_{\mathbf{k}} + i\tilde{\eta}''_{\mathbf{k}}$. In Eq. (38), the first term proportional to $\tilde{\eta}'_{\mathbf{k}}^2$ corresponds to the amplitude fluctuations while the second term proportional to $\tilde{\eta}''_{\mathbf{k}}^2$

corresponds to the phase fluctuations [34]. By setting $\psi_0^{(\text{GF})} = 0$, Eq. (38) recovers Eq. (26) for $T \geq T_c$. The contribution of thermal fluctuations to the free energy below T_c is obtained as

$$\begin{aligned} F_{\text{fl}}^- &= -\frac{1}{\beta} \ln \int \mathcal{D}[\eta(\mathbf{r})] e^{-\beta F_{\eta}^{\text{Popov}}[\eta(\mathbf{r})]} \\ &= -\frac{1}{2\beta} \sum_{\mathbf{k}} \left[\ln \left(\frac{\pi k_B T}{a(T) + 2b\langle|\eta|^2\rangle + 3b(\psi_0^{(\text{GF})})^2 + \gamma k^2} \right) \right. \\ &\quad \left. + \ln \left(\frac{\pi k_B T}{a(T) + 2b\langle|\eta|^2\rangle + b(\psi_0^{(\text{GF})})^2 + \gamma k^2} \right) \right]. \end{aligned} \quad (39)$$

The thermal average of the GF is self-consistently determined by

$$\begin{aligned} \langle|\eta|^2\rangle &= \frac{1}{\mathcal{Z}_{\eta}} \int \mathcal{D}[\eta(\mathbf{r})] |\eta(\mathbf{r})|^2 e^{-\beta F_{\eta}^{\text{Popov}}[\eta(\mathbf{r})]} \\ &= \frac{1}{2\beta L^2} \sum_{\mathbf{k}} \left[\frac{1}{a(T) + 2b\langle|\eta|^2\rangle + 3b(\psi_0^{(\text{GF})})^2 + \gamma k^2} \right. \\ &\quad \left. + \frac{1}{a(T) + 2b\langle|\eta|^2\rangle + b(\psi_0^{(\text{GF})})^2 + \gamma k^2} \right]. \end{aligned} \quad (40)$$

Above T_c in which $\psi_0^{(\text{GF})} = 0$, the two contributions from amplitude and phase fluctuations become identical and Eq. (40) recovers Eq. (30). The temperature dependences of $\langle|\eta|^2\rangle$ and the temperature derivative are shown in Fig. 2. We numerically find that $\langle|\eta|^2\rangle$ including the GF determined by Eq. (30) can exhibit a slight discontinuity at T_c as $\langle|\eta|^2\rangle_{T \rightarrow T_c^-} < \langle|\eta|^2\rangle_{T \rightarrow T_c^+}$. Nonetheless, the deviation $\langle|\eta|^2\rangle_{T \rightarrow T_c^+} - \langle|\eta|^2\rangle_{T \rightarrow T_c^-}$ is decreased with a smaller Gi and we set $\text{Gi} = 0.1 \ll 1$ so that the deviation is negligible. See Appendix A for details. The quasi-order parameter (19) including GF determined by Eq. (40) is shown in Fig. 1 by a dashed green curve. With Eq. (33), the quasi-order parameter (19) including the GF in the vicinity of T_c can be written as

$$(\psi_0^{(\text{GF})})^2 = \frac{\alpha k_B}{b} A_{-}(T_c - T), \quad (41)$$

with

$$A_{\pm} \equiv 1 + \frac{2b}{\alpha k_B} \partial_T \langle|\eta|^2\rangle \Big|_{T \rightarrow T_c^{\pm}}, \quad (42)$$

which are directly related to the temperature derivative of $\langle|\eta|^2\rangle$ shown in the inset of Fig. 2. The coefficient A_{-} in Eq. (41) reflects the Gaussian correction by $\langle|\eta|^2\rangle$.

V. TOPOLOGICAL DEFECTS IN THE PHASE OF THE QUASI-ORDER PARAMETER WITH GAUSSIAN FLUCTUATIONS

Let us write the space-dependent quasi-order parameter as

$$\begin{aligned} \psi(\mathbf{r}) &= \left[\psi_0^{(\text{BKT})} + \sigma(\mathbf{r}) \right] e^{i\theta_0(\mathbf{r}) + i\theta(\mathbf{r})} \\ &\simeq \left[\psi_0^{(\text{BKT})} + \eta(\mathbf{r}) \right] e^{i\theta(\mathbf{r})}, \end{aligned} \quad (43a)$$

$$\eta(\mathbf{r}) = |\eta(\mathbf{r})| e^{i\phi(\mathbf{r})}, \quad (43b)$$

with $\eta(\mathbf{r}) = \sigma(\mathbf{r}) + i\theta_0(\mathbf{r})\psi_0^{(\text{BKT})}$ including both amplitude and phase fluctuations to the first order where $\theta_0(\mathbf{r})$ and $\phi(\mathbf{r})$ being the regular phases with zero winding number. The phase field $\theta(\mathbf{r})$ takes into account phase fluctuations with quantized vortices. The compactness of the phase angle field $\theta(\mathbf{r})$ implies

$$\oint_{\mathcal{C}} \nabla \theta(\mathbf{r}) \cdot d\mathbf{r} = 2\pi q \quad (44)$$

for any closed contour \mathcal{C} . Here, $q = 0, \pm 1, \pm 2, \dots$ is the integer topological charge associated with the corresponding quantized vortex (positive q) or antivortex (negative q). Inserting Eq. (43a) into Eq. (2), one obtains

$$F_s = F_{s0}^{(\text{BKT})} + F_{\eta} + F_{\theta}, \quad (45)$$

with

$$\begin{aligned} F_{\eta} &\equiv \int d^2\mathbf{r} \left[\left[a(T) + 2b(\psi_0^{(\text{BKT})})^2 + \gamma(\nabla\tilde{\theta})^2 \right] |\eta(\mathbf{r})|^2 \right. \\ &\quad \left. + \frac{b}{2} |\eta(\mathbf{r})|^4 + \frac{b}{2} (\psi_0^{(\text{BKT})})^2 [\eta(\mathbf{r})^2 + \eta^*(\mathbf{r})^2] \right. \\ &\quad \left. + b\psi_0 \left[(\psi_0^{(\text{BKT})})^2 + |\eta(\mathbf{r})|^2 \right] [\eta(\mathbf{r}) + \eta^*(\mathbf{r})] + \gamma |\nabla\eta(\mathbf{r})|^2 \right], \end{aligned} \quad (46)$$

which recovers F_{η}^{Popov} in Eq. (38) under the Popov approximation by taking the thermal average and neglecting $(\nabla\tilde{\theta})^2$, and

$$\begin{aligned} F_{\theta} &\equiv \gamma \int d^2\mathbf{r} \left[(\psi_0^{(\text{BKT})})^2 (\nabla\tilde{\theta})^2 \right. \\ &\quad \left. + 2\psi_0^{(\text{BKT})} (\nabla\theta)^2 \text{Re}[\eta(\mathbf{r})] + 2\psi_0^{(\text{BKT})} \nabla\theta \cdot \nabla \text{Im}[\eta(\mathbf{r})] \right. \\ &\quad \left. + \frac{1}{4(\psi_0^{(\text{BKT})})^2} [\eta(\mathbf{r}) \nabla\eta^*(\mathbf{r}) - \eta^*(\mathbf{r}) \nabla\eta(\mathbf{r})]^2 \right], \end{aligned} \quad (47)$$

which involves $\theta(\mathbf{r})$ and

$$\tilde{\theta}(\mathbf{r}) \equiv \theta(\mathbf{r}) + \frac{\langle|\eta|^2\rangle}{(\psi_0^{(\text{BKT})})^2} \phi(\mathbf{r}). \quad (48)$$

The last line in Eq. (47) is the higher-order contribution in $\eta(\mathbf{r})$ which is neglected in the following.

From Eq. (47), the equation of motion in terms of θ reads

$$0 = -\gamma(\psi_0^{(\text{BKT})})^2(\nabla\tilde{\theta})^2 + \gamma\psi_0^{(\text{BKT})}[\eta(\mathbf{r}) + \eta^*(\mathbf{r})]\nabla^2\theta - i\gamma\psi_0^{(\text{BKT})}[\nabla^2\eta^*(\mathbf{r}) - \nabla^2\eta(\mathbf{r})]. \quad (49)$$

By performing the thermal average with respect to η on the equation of motion (49), one may obtain

$$0 = \gamma(\psi_0^{(\text{BKT})})^2\nabla^2\tilde{\theta} = \frac{\delta F_\theta^{\text{Popov}}}{\delta\theta}, \quad (50)$$

where

$$F_\theta^{\text{Popov}} \equiv \frac{J_0(T)}{2} \int d^2\mathbf{r} (\nabla\tilde{\theta})^2 \quad (51)$$

is the XY free energy under the Popov approximation generating Eq. (50) with $J_0(T) \equiv 2\gamma(\psi_0^{(\text{BKT})})^2$ being the bare phase stiffness. Note that $\tilde{\theta}(\mathbf{r})$ in Eq. (48) keeps the circulation of vorticity invariant from that of $\theta(\mathbf{r})$ because $\phi(\mathbf{r})$ is regular. The equation of motion with respect to $\psi_0^{(\text{BKT})}$ reads

$$0 = \frac{\delta F_s}{\delta\psi_0^{(\text{BKT})}} = 2\psi_0^{(\text{BKT})} \left[a(T) + b(\psi_0^{(\text{BKT})})^2 + 2b|\eta(\mathbf{r})|^2 + \gamma(\nabla\tilde{\theta}(\mathbf{r}))^2 \right]. \quad (52)$$

Here, we neglected the anomalous terms of $\eta(\mathbf{r})$ which vanish with the thermal average. Performing the thermal average with respect to $F_s^{\text{Popov}} = F_{s0}^{(\text{BKT})} + F_\eta^{\text{Popov}} + F_\theta^{\text{Popov}}$ with

$$\frac{F_{s0}^{(\text{BKT})}}{L^2} = \left[a(T) + 2b\langle|\eta|^2\rangle + \gamma\langle(\nabla\tilde{\theta})^2\rangle \right] (\psi_0^{(\text{BKT})})^2 + \frac{b}{2}(\psi_0^{(\text{BKT})})^4, \quad (53)$$

one obtains

$$(\psi_0^{(\text{BKT})})^2 = -\frac{a(T) + 2b\langle|\eta|^2\rangle + \gamma\langle(\nabla\tilde{\theta})^2\rangle}{b}, \quad (54)$$

if $a(T) + 2b\langle|\eta|^2\rangle + \gamma\langle(\nabla\tilde{\theta})^2\rangle \geq 0$ where $\langle|\eta|^2\rangle$ is given by $\langle|\eta|^2\rangle = \int \mathcal{D}[\eta(\mathbf{r})]|\eta(\mathbf{r})|^2 \exp[-\beta F_\eta^{\text{Popov}}[\eta(\mathbf{r})]]/\mathcal{Z}_\eta$ and $\langle(\nabla\tilde{\theta})^2\rangle$ can be evaluated as

$$\langle(\nabla\tilde{\theta})^2\rangle = \frac{1}{\mathcal{Z}_\theta} \int \mathcal{D}[\tilde{\theta}(\mathbf{r})] (\nabla\tilde{\theta}(\mathbf{r}))^2 e^{-\beta F_\theta^{\text{Popov}}} = \frac{\Lambda^2 - k_0^2}{4\pi K_0(T)}, \quad (55)$$

with $\mathcal{Z}_\theta \equiv \int \mathcal{D}[\tilde{\theta}(\mathbf{r})] e^{-\beta F_\theta^{\text{Popov}}}$ and $K_0(T) = \beta J_0(T)$. In the high-temperature regime in which $a(T) + 2b\langle|\eta|^2\rangle +$

$\gamma\langle(\nabla\tilde{\theta})^2\rangle < 0$, $\psi_0^{(\text{BKT})} = 0$. Inserting Eq. (55) into Eq. (54), we determine ψ_0 in Eq. (54) and the bare superfluid phase stiffness $J_0(T)$. By solving Eq. (55) with respect to $\langle(\nabla\tilde{\theta})^2\rangle$, one obtains $\langle(\nabla\tilde{\theta})^2\rangle = [-a(T) - 2b\langle|\eta|^2\rangle - \sqrt{D}]/2\gamma$. Unfortunately, it has a real root only in the low-temperature regime in which $D \equiv [-a(T) - 2b\langle|\eta|^2\rangle]^2 - b(\Lambda^2 - k_0^2)/2\pi\beta \geq 0$ holds. Then, in the high-temperature regime in which $D < 0$, we assume $\langle(\nabla\tilde{\theta})^2\rangle = [-a(T) - 2b\langle|\eta|^2\rangle]/2\gamma$, which vanishes at T_c by neglecting the imaginary part. Consequently, in the high-temperature regime of $D < 0$, we have $\psi_0^{(\text{BKT})} = \psi_0^{(\text{GF})}/\sqrt{2}$.

As shown by Kosterlitz and Thouless [7], in the two-dimensional case, the total number of quantized vortices varies as a function of the temperature: at zero temperature there are no vortices, however as the temperature increases vortices start to appear in vortex-antivortex pairs. The phase stiffness is renormalized by the presence of these vortex-antivortex pairs. The pairs are bound at low temperatures, until at the BKT critical temperature T_{BKT} an unbinding transition occurs above which a proliferation of free vortices and antivortices is observed. At T_{BKT} the renormalized phase stiffness $J_R(T)$ jumps to zero and for $T > T_{\text{BKT}}$ the superfluidity is completely lost. Moreover, the renormalized free energy becomes

$$F_s^{\text{Popov}} = F_{s0}^{(\text{BKT})}[\psi_R^{\text{BKT}}] + F_\eta^{\text{Popov}}[\psi_R^{\text{BKT}}] + \int d^2\mathbf{r} \frac{J_R(T)}{2} |\nabla\tilde{\theta}(\mathbf{r})|^2 \quad (56)$$

where

$$\psi_R^{\text{BKT}}(T) = \sqrt{\frac{J_R(T)}{2\gamma}}. \quad (57)$$

We now discuss how one can obtain the renormalized phase stiffness $J_R(T)$ from the bare one $J_0(T)$. The NK renormalization group equations are given by [7]

$$\partial_l K_l(T)^{-1} = 4\pi^3 y_l(T)^2 \quad (58)$$

$$\partial_l y_l(T) = [2 - \pi K_l(T)] y_l(T) \quad (59)$$

where l is the running RG scale, which goes from $l = 0$ (bare results) to $l = l_{\text{max}} = \ln(\pi/\xi k_0)$ (fully renormalized results),

$$J_l(T) = k_B T K_l(T) \quad (60)$$

is the running phase stiffness, and

$$\mu_l(T) = -k_B T \ln y_l(T) \quad (61)$$

is the running vortex-core energy. We can obtain the fully renormalized phase stiffness $J_R(T) = J_{l_{\text{max}}}(T)$ and the fully renormalized vortex-core energy $\mu_R(T) = \mu_{l_{\text{max}}}(T)$.

Quite remarkably, by separation of variables, from Eqs. (58) and (59) one finds [43]

$$y_l(T)^2 - \frac{1}{\pi^3 K_l(T)} - \frac{1}{2\pi^2} \ln K_l(T) = C, \quad (62)$$

where C is an integration constant, determined by the initial conditions. For the critical trajectory, where $T = T_{\text{BKT}}$, one has $y_{\text{R}}(T_{\text{BKT}}) = 0$ and $K_{\text{R}}(T_{\text{BKT}}) = 2/\pi$, namely

$$k_{\text{B}}T_{\text{BKT}} = \frac{\pi}{2}J_{\text{R}}(T_{\text{BKT}}^-). \quad (63)$$

In addition, from Eq. (62) and the previous expressions, one also obtains for the critical trajectory [43]

$$C = \frac{\ln(\pi/2) - 1}{2\pi^2} = -0.0278. \quad (64)$$

It is important to stress that Eq. (63) relates the BKT critical temperature T_{BKT} to the fully renormalized phase stiffness $J_{\text{R}}(T_{\text{BKT}})$ calculated at the same BKT critical temperature. Sometimes, one uses an approximated version of Eq. (63), the so-called NK criterion [8], substituting $J_{\text{R}}(T_{\text{BKT}}^-)$ with $J_0(T_{\text{BKT}}^-)$. In this way, one quickly gets an approximated T_{BKT} from the knowledge of the bare superfluid density $J_0(T)$. Here, however, we improve this approximation. For the initial condition of the vortex core energy we choose

$$\mu_0(T) = \frac{\pi^2}{4}J_0(T), \quad (65)$$

that is currently the most rigorous choice for superconductors and superfluids [44–47]. As a consequence, the initial condition of the vortex fugacity reads

$$y_0(T) = e^{-\pi^2 K_0(T)/4}. \quad (66)$$

Consequently, at the BKT critical temperature from Eqs. (62), (64), and (66) we have

$$\begin{aligned} \frac{2}{\pi K_0(T_{\text{BKT}})} - \ln\left(\frac{2}{\pi K_0(T_{\text{BKT}})}\right) - 2\pi^2 e^{-\pi^2 K_0(T_{\text{BKT}})/2} \\ = 1. \end{aligned} \quad (67)$$

The unknown $K_0(T_{\text{BKT}})$ can be then found by solving numerically the above equation, obtaining

$$K_0(T_{\text{BKT}}) = 1.055 \quad (68)$$

or, equivalently, from $K_0(T_{\text{BKT}}) = J_0(T_{\text{BKT}})/(k_{\text{B}}T_{\text{BKT}})$, the remarkable semi-analytical result [60]

$$k_{\text{B}}T_{\text{BKT}} = 0.948 J_0(T_{\text{BKT}}). \quad (69)$$

This formula is much simpler than Eq. (63) because it depends only on the knowledge of the bare phase stiffness $J_0(T)$. Moreover, it is much more reliable than the approximated NK criterion discussed earlier.

Several theoretical studies beyond perturbative RG analysis revealed that the RG equations (58) and (59) are not subject to modification due to the coupling with the Higgs mode by redefining the vortex fugacity including a constant factor [51–56]. Based on this knowledge, we keep using the RG equations but with the bare quantities given by $K_0(T) = 2\gamma(\psi_0^{(\text{BKT})})^2$ and $y_0(T) = \exp[-\pi^2 K_0(T)/4]$ determined from Eq. (54) which encodes the coupling with the Higgs mode.

Using the renormalized phase stiffness $K_{\text{R}}(T) = 2\gamma(\psi_{\text{R}}^{(\text{BKT})})^2$ and vortex fugacity $y(T)$, we can obtain the effective free energy by integrating out $\tilde{\theta}$ in Eq. (51) as

$$\begin{aligned} F_{\text{fl,XY}} &= -\frac{1}{\beta} \ln \int \mathcal{D}[\tilde{\theta}(\mathbf{r})] e^{-\beta F_{\theta}^{\text{Popov}}} \\ &= -\frac{1}{\beta} \sum_{\mathbf{k}} \ln \left(\frac{2\pi}{K_{\text{R}}(T)k^2} \right). \end{aligned} \quad (70)$$

As in Eq. (39), the integration of $\eta(\mathbf{r})$ results in

$$\begin{aligned} F_{\text{fl}}^- &= -\frac{1}{\beta} \ln \int \mathcal{D}[\eta(\mathbf{r})] e^{-\beta F_{\eta}^{\text{Popov}}[\eta(\mathbf{r})]} \\ &= -\frac{1}{2\beta} \sum_{\mathbf{k}} \left[\ln \left(\frac{\pi k_{\text{B}}T}{a(T) + 2b\langle|\eta|^2\rangle + \gamma\langle(\nabla\tilde{\theta})^2\rangle + 3b(\psi_{\text{R}}^{(\text{BKT})})^2 + \gamma k^2} \right) \right. \\ &\quad \left. + \ln \left(\frac{\pi k_{\text{B}}T}{a(T) + 2b\langle|\eta|^2\rangle + \gamma\langle(\nabla\tilde{\theta})^2\rangle + b(\psi_{\text{R}}^{(\text{BKT})})^2 + \gamma k^2} \right) \right]. \end{aligned} \quad (71)$$

In the normal phase in which $\psi_{\text{R}}^{(\text{BKT})} = 0$, F_{fl}^+ is given by Eq. (28) and we neglect $F_{\text{fl,XY}}$ because we have $F_{\theta}[\psi_0 = \psi_{\text{R}}^{(\text{BKT})}] = 0$.

The superfluid phase transition temperatures scaled by the Fermi temperature are summarized in Fig. 3.

In Fermi systems, a larger value of $\text{Gi} = \pi T_{\text{c}0}/2T_{\text{F}}$ corresponds to a stronger pairing interaction. In our Ginzburg-Landau problem, when the bare phase stiffness

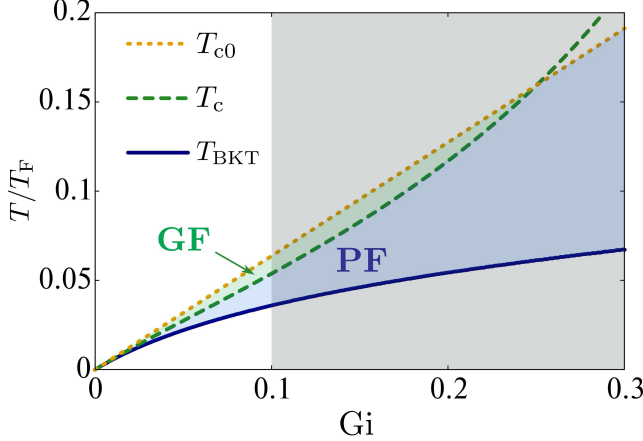


FIG. 3. Dependence of the critical temperatures T_{c0} , T_c , and T_{BKT} in the unit of T_F on Gi . The gray region $Gi \gtrsim 0.1$ is the unphysical region in which T_c/T_{c0} increases in terms of Gi . The shaded region of $T_c < T < T_{c0}$ is governed by the Gaussian thermal fluctuations (GF), while the phase fluctuations (PF) associated with vortex excitations are dominant in the region of $T_{\text{BKT}} < T < T_c$.

in the vicinity of T_c is given by

$$J_0(T) = \frac{k_B}{2\pi Gi} A_-(T_c - T), \quad (72)$$

we obtain

$$\frac{T_c - T_{\text{BKT}}}{T_{\text{BKT}}} = \frac{2\pi}{0.948 A_-} Gi \quad (73)$$

with Gi the Ginzburg-Levanyuk number defined by Eq. (34) and A_- is defined by Eq. (42). The formula (73) is valid if the BKT transition temperature is close to T_c at which the linear approximation of the phase stiffness in Eq. (72) holds, corresponding to $Gi \ll 1$. Without Gaussian fluctuations, Eq. (73) reduces to

$$\frac{T_{c0} - T_{\text{BKT},0}}{T_{\text{BKT},0}} = \frac{2\pi}{0.948} Gi, \quad (74)$$

where $T_{\text{BKT},0}$ represents the BKT transition temperature without the Gaussian thermal fluctuations. The dotted-dashed gray curve in Fig. 1 represents the quasi-order parameter without Gaussian fluctuations. The obtained BKT transition temperature (73) is lower than the upper bound $T_F/8$ for $Gi \lesssim 0.4$ under $A_- \simeq 1$ [33]. Figure 3 also reveals that the ratio between the GF and MF critical temperatures T_c/T_{c0} swells with a large Gi , which is unphysical because fluctuations must tend to break ordered phase lowering the transition temperature. The gray region in Fig. 3 represents the unphysical region in which T_c/T_{c0} increases with respect to Gi . Therefore, we can identify $Gi \lesssim 0.1$ as the regime in which our Ginzburg-Landau analysis is physically reasonable.

The effects of fluctuations on the transition temperature are summarized in Fig. 1. It shows the quasi-order

parameters $|\psi_0|^2 = \alpha k_B(T_{c0} - T)/b$ within the MF level in Eq. (11), $|\psi_0^{(\text{GF})}|^2 = -a(T)/b - 2\langle|\eta|^2\rangle$ at the GF level, and $|\psi_R^{(\text{BKT})}|^2 = J_R(T)/2\gamma$ including the vortex excitations. Including the GF without vortex excitations decreases the T_{c0} to T_c as in Eq. (36). The PF associated with the vortex excitations further reduce the critical temperature from T_c to $T_{\text{BKT},0}$, and the coupling with the Higgs mode reduces $T_{\text{BKT},0}$ to T_{BKT} as reported in Fig. 1.

VI. MAGNETIC PROPERTIES

In this section, we show the magnetic properties by focusing on the penetration depth and the critical magnetic fields.

A. Penetration depth

Adopting the saddle-point approximation with respect to the appropriate free energy functional, one can deduce the London penetration depth [40, 49]

$$\lambda(T) = \sqrt{\frac{b}{2\mu_0 Q^2 \gamma a(T)}} = \sqrt{\frac{1}{2\mu_0 Q^2 \gamma |\psi_0(T)|^2}} \quad (75)$$

of the magnetic field at the MF level, at the GF level, and also at the BKT level by substituting ψ_0 with $\psi_0^{(\text{GF})}$ and $\psi_R^{(\text{BKT})}$ where Q is the electrical charge and μ_0 is the magnetic constant.

Having the London penetration depth $\lambda(T)$ and the Ginzburg-Landau coherence length

$$\xi(T) = \sqrt{\frac{\gamma}{|a(T)|}} = \sqrt{\frac{\gamma}{b|\psi_0(T)|^2}}, \quad (76)$$

one immediately finds the Ginzburg-Landau parameter

$$\kappa = \frac{\lambda(T)}{\xi(T)} = \sqrt{\frac{b}{2\mu_0 Q^2 \gamma^2}}, \quad (77)$$

such that $\kappa < 1/\sqrt{2}$ for type-I superconductors and $\kappa > 1/\sqrt{2}$ for type-II superconductors [49]. We determine the quasi-order parameters in Eqs. (75) and (76) by the saddle-point of the free energy in Eq. (9) within the MF level, Eq. (21) including GF, and Eqs. (58) and (59) including the vortex excitations responsible for the BKT transition. The GL parameter is independent of the order parameter and temperature by definition of Eq. (77). BKT transitions can be discussed in type-II superconductors and we focus on them in the following [50].

The coherence length in Eq. (76) also represents the vortex core size. According to Fig. 1, Eq. (76) implies that the vortex core size becomes larger by taking into account thermal fluctuations.

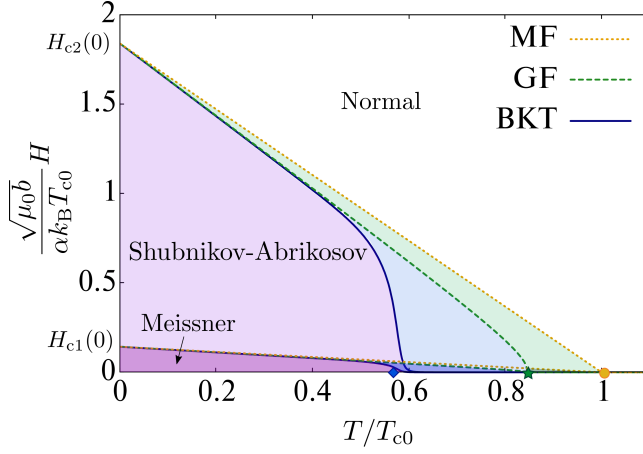


FIG. 4. H - T phase diagram of a type-II superconductor within the MF level, including the GF, and the vortex excitations, respectively. The critical magnetic fields are given by Eqs. (83) with Eqs. (79), (81), and (82) respectively for $Gi = 0.1$ and $\kappa = 1.3$. The phase in the region $0 < H < H_{c1}$ is the Meissner phase while the one in $H_{c1} < H < H_{c2}$ is the Shubnikov-Abrikosov phase [49].

B. Critical magnetic field

At the MF level, the thermodynamic critical magnetic field H_c is related to the free energy as [49]

$$F_{s0} = -L^2 \frac{\mu_0}{2} H_c^2. \quad (78)$$

It follows that the critical magnetic field reads [49]

$$\begin{aligned} H_c(T) &= \sqrt{\frac{2}{\mu_0} \left| a(T) \psi_0^2(T) + \frac{b}{2} \psi_0(T)^4 \right|} \\ &= \sqrt{\frac{b}{\mu_0}} \psi_0(T)^2 = \frac{\alpha k_B}{\sqrt{\mu_0 b}} (T_{c0} - T). \end{aligned} \quad (79)$$

We now include the effects of fluctuations in the calculation of the critical magnetic field. However, adopting the saddle-point approximation, we use instead Eq. (21) as

$$F_{s0}^{(GF)} = -L^2 \frac{\mu_0}{2} (H_c^{(GF)})^2, \quad (80)$$

and the critical magnetic field is given by

$$H_c^{(GF)}(T) = \sqrt{\frac{b}{\mu_0}} \left(\psi_0^{(GF)} \right)^2. \quad (81)$$

with Eq. (19). By including the vortex excitations and adopting a similar saddle-point approximation on the BKT free energy (53), the critical magnetic field is subject to renormalization as

$$H_c^{(BKT)}(T) = \sqrt{\frac{b}{\mu_0}} \left(\psi_R^{(BKT)} \right)^2. \quad (82)$$

With the Ginzburg-Landau parameter κ , the critical magnetic fields H_{c1} and H_{c2} of type-II superconductors are deduced from H_c by using the formulas [49]

$$H_{c1}(T) = \frac{1}{\sqrt{2}} \frac{\ln(\kappa)}{\kappa} H_c(T), \quad (83a)$$

$$H_{c2}(T) = \sqrt{2\kappa} H_c(T). \quad (83b)$$

Here, the expression of Eq. (83a) is valid only with $\kappa \gg 1/\sqrt{2}$ [49]. Figure 4 shows the H - T phase diagram within the MF level and the beyond-MF level including GF, and vortex excitations, respectively, for $Gi = 0.1$. We used the GL parameter $\kappa = 1.3$, which is the typical value in Nb superconductors [49]. The phase in the region $0 < H < H_{c1}$ is the Meissner phase while the one in $H_{c1} < H < H_{c2}$ is the Shubnikov-Abrikosov phase [49].

VII. HEAT CAPACITY

From the free energy, one can also determine the size of the discontinuous jump in the heat capacity at the superfluid phase transition point as [34]

$$\Delta C = -\frac{T}{L^2} \frac{\partial^2 F_s}{\partial T^2}. \quad (84)$$

First, we start with a recap of the mean-field case plus the thermal fluctuations, which is exactly the case considered in Ref. [34]. The contribution from the thermal fluctuations F_{fl} can be singular while that from F_{s0} is regular. In the vicinity of T_{c0} , the heat capacity due to the thermal fluctuations reads

$$\Delta C_{fl,MF}^{\pm} = -\frac{T}{L^2} \frac{\partial^2 F_{fl,MF}^{\pm}}{\partial T^2} \quad (85)$$

By focusing only on the most singular part in Eq. (85) in the vicinity of the superfluid phase transition temperature, a straightforward calculation yields (see Appendix B)

$$\Delta C_{fl,MF}^{-} = \Delta C_{fl,MF}^{+}, \quad (86)$$

if $\xi\Lambda \rightarrow \infty$ and $\xi k_0 \rightarrow 0$. Otherwise, the relation (86) no longer holds. Consequently, the heat capacity exhibits no jump at the superfluid phase transition under $Gi \rightarrow 0$ within the mean-field level in 2D [34].

By including the GF, we obtain

$$\Delta C_{fl,GF}^{-} = \left(\frac{A_{-}}{A_{+}} \right)^3 \Delta C_{fl,GF}^{+}, \quad (87)$$

if $\xi\Lambda \rightarrow \infty$ and $\xi k_0 \rightarrow 0$. Otherwise, the relation (87) no longer holds. In contrast to the MF case in Eq. (86), Eq. (87) implies that the heat capacity can exhibit discontinuity at the superfluid transition point even with

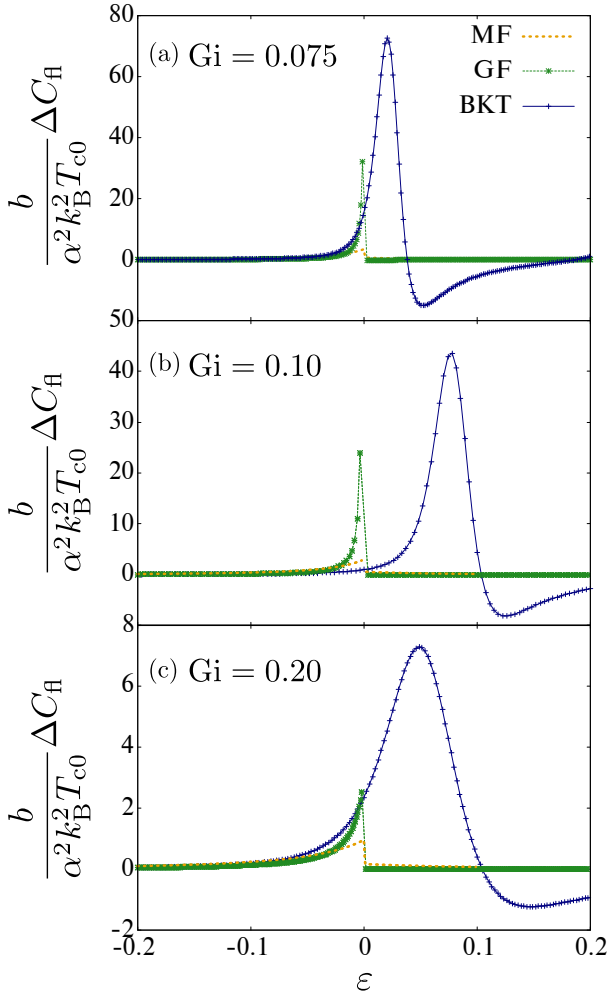


FIG. 5. Fluctuation contributions to the heat capacity ΔC_{fl} as a function of the reduced temperature $\varepsilon = (T - T_{\text{c}0})/T_{\text{c}0}$ (MF), $(T - T_{\text{c}})/T_{\text{c}}$ (GF), $(T - T_{\text{BKT}})/T_{\text{BKT}}$ (BKT) with $\text{Gi} = 0.075$ (a), 0.1 (b), 0.2 (c).

$\xi\Lambda \rightarrow \infty$ and $\xi k_0 \rightarrow 0$ due to the Gaussian corrections in A_{\pm} .

Figure 5 shows the heat capacity due to the fluctuation contribution $\Delta C_{\text{fl}} = -T\partial^2 F_{\text{fl}}^{\pm}/\partial T^2/L^2$ with three different values of the Ginzburg-Levanyuk number Gi , which may exhibit singular behavior at the transition temperature, with respect to the reduced temperature

$$\varepsilon = \begin{cases} \frac{T - T_{\text{c}0}}{T_{\text{c}0}} & (\text{MF}), \\ \frac{T - T_{\text{c}}}{T_{\text{c}}} & (\text{GF}), \\ \frac{T - T_{\text{BKT}}}{T_{\text{BKT}}} & (\text{BKT}). \end{cases} \quad (88)$$

In both MF and GF levels, the heat capacity exhibits a discontinuity at criticality $\varepsilon = 0$. This is consistent with our analytic calculation in Appendix B. Indeed, we

are working with a finite momentum cutoff $k_0 > 0$ and the continuous behavior of the heat capacity in a 2D superconductor within the MF level can be obtained only under the condition $\xi k_0 \rightarrow 0$ as well as $\xi\Lambda \rightarrow \infty$. On the other hand, by taking into account the BKT transition, the heat capacity shows no singularity at $\varepsilon = 0$. This continuous change originates from the smooth behavior of the quasi-order parameter at T_{BKT} shown in Fig. 1 and reflects the infinite-order phase transition [24]. Instead, it exhibits a maximum above the BKT transition temperature for any values of Gi , which is consistent with a numerical prediction [24]. The contribution of phase fluctuations in Eq. (70) is mainly responsible for the behavior of ΔC_{fl} . In other words, the measurement of the heat capacity around the critical temperature can be useful to verify the BKT transition in a finite-size superconducting material [19]. For instance, Mizukami *et al.* reported a BCS-like jump of the heat capacity at the superconducting transition temperature in the nematic phase of $\text{FeSe}_{1-x}\text{S}_x$, when $x < 0.17$ [20]. This can be attributed to the dimensionality of the sample that is not strictly 2D and thus, Gaussian fluctuations are dominating over the topological ones giving the typical jump in the heat capacity at the transition temperature. We suggest that the change in behavior of the heat capacity can be used to detect the transition from the 3D to the 2D regime when the thickness of the sample is reduced. However, upon entering the tetragonal phase at $x > 0.17$, where nematic order is suppressed, the discontinuous jump of the heat capacity at the critical temperature disappears. This has been attributed to a reminiscence of the BEC transition in Bose gas systems, so in this regime, the continuity of the heat capacity at the transition is due to other effects rather than dimensionality. In this phase, highly non-mean-field behaviors consistent with BEC-like pairing are found in the thermodynamic quantities with giant superconducting fluctuations extending far above T_{c} . The broadening of the peak in the heat capacity at the superconducting transition when the system is tuned toward the crossover and the BEC regime of the BCS-BEC crossover observed in experiments is compatible with our results in Fig. 5. A larger Gi decreases the RG cutoff $l_{\text{max}} = \ln(\pi/\xi k_0)$ smearing the jump of the phase stiffness, which results in the broadening of the heat capacity as shown in Fig. 5. With $\text{Gi} = 0.075$ shown in Fig. 5(a), the maximum of the BKT heat capacity is closer to $\varepsilon = 0$ than the one with $\text{Gi} = 0.1$ plotted in Fig. 5(b) and the behaviors of the GF and BKT heat capacities in the superfluid phase $\varepsilon < 0$ are almost indistinguishable. However, the maximum of the BKT heat capacity above T_{BKT} makes the behaviors in the normal phase $\varepsilon > 0$ dramatically different. Compared with Fig. 5(c), we can also observe that the heat capacity is suppressed as well as broadened by a large value of Gi . It demonstrates that a smaller infrared momentum cutoff $k_0 = (\text{Gi}k_B T_c/\gamma)^{1/2}$ enhances the heat capacity not only at the GF level (see Eqs. (B12)) but also at the BKT level.

VIII. CONCLUSIONS

In conclusion, we performed the Ginzburg-Landau analysis to reveal that the mean-field critical temperature T_{c0} of the Ginzburg-Landau functional is reduced by Gaussian fluctuations according to Eq. (36). Then, it is further reduced by vortex excitations according to Eq. (73). We incorporated the effects of both amplitude fluctuations and phase fluctuations associated with vortex-antivortex excitations responsible for the BKT transition. With the semi-analytic relation between the bare superfluid phase stiffness and the renormalized one, we obtained a formula for the shift of the transition temperature including the topological vortex-antivortex excitations. Based on our approach to the cascade of fluctuations, we obtained the H - T phase diagram of type-II superconductors and the critical behaviors of the heat capacity. The singular behavior of the heat capacity at criticality is hindered by phase fluctuations associated with the vortex-antivortex excitations, which is useful to verify which types of fluctuations dominate in a two-dimensional superconducting material.

The Ginzburg-Landau theory is capable of describing multicomponent systems such as multiband superconductors as well as the single-component ones studied in this manuscript. In particular, the BKT transition is subject to change qualitatively due to the multicomponent character [57–61]. The clarification of the roles of fluctuations and their temperature evolution in the multicomponent two-dimensional superconductivity or superfluidity by extending this work to include multichannel fluctuations would be of great interest [39].

Appendix A: Determination of $\langle|\eta|^2\rangle$

The self-consistent equation (40) determines $\langle|\eta|^2\rangle$. Figure 6 shows a plot of

$$g[\langle|\eta|^2\rangle(T)] \equiv \langle|\eta|^2\rangle - \frac{k_B T}{8\pi\gamma} \ln \left(\frac{1}{4\text{Gi}} \frac{2\alpha k_B(T_{c0} - T) - 4b\langle|\eta|^2\rangle + \alpha k_B T_c/4}{2\alpha k_B(T_{c0} - T) - 4b\langle|\eta|^2\rangle + \text{Gi}\alpha k_B T_c} \right), \quad (\text{A1})$$

with $\text{Gi} = 0.1$. Equation (40) equivalent to $g[\langle|\eta|^2\rangle(T)] = 0$ determines $\langle|\eta|^2\rangle$. There are two roots of Eq. (40) for $\langle|\eta|^2\rangle_c - \langle|\eta|^2\rangle \leq 0$ and $\langle|\eta|^2\rangle_c - \langle|\eta|^2\rangle > 0$ respectively with $\langle|\eta|^2\rangle_c \equiv \langle|\eta|^2\rangle_{T \rightarrow T_c^+}$ defined by Eq. (32). The former is an unphysical root (open circles in Fig. 6) and the latter that vanishes at zero temperature is what we obtained to illustrate the quasi-order parameter in Fig. 1 (filled red points in Fig. 6). However, the self-consistent equation (A1) reveals that $\langle|\eta|^2\rangle = \langle|\eta|^2\rangle_c$ at $T = T_c$ is satisfied only by the unphysical root and the physical root still has a deviation $\langle|\eta|^2\rangle_{T \rightarrow T_c^-} > \langle|\eta|^2\rangle_c$ as shown in Fig. 6. This deviation of $\langle|\eta|^2\rangle_{T \rightarrow T_c^-}$ from $\langle|\eta|^2\rangle_c$ is diminished by a smaller Gi and vanishes in $\text{Gi} \rightarrow 0$. To

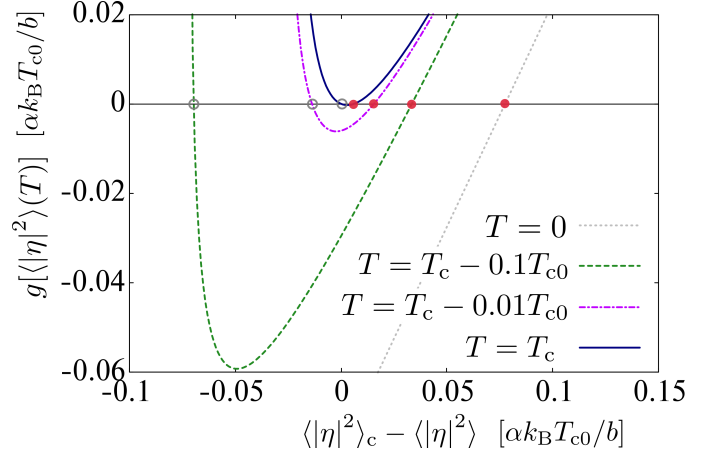


FIG. 6. Plot of $g[\langle|\eta|^2\rangle]$ in Eq. (A1) with respect to $\langle|\eta|^2\rangle_c - \langle|\eta|^2\rangle$ below T_c with $\text{Gi} = 0.1$. The zero point corresponds to the root of Eq. (40). The filled red points satisfying $\langle|\eta|^2\rangle_c - \langle|\eta|^2\rangle \geq 0$ are physical roots, while the open circles in the region of $\langle|\eta|^2\rangle_c - \langle|\eta|^2\rangle \leq 0$ are unphysical roots.

consider the region in which the deviation is negligible, we consider $\text{Gi} = 0.1 \ll 1$ throughout this work.

Appendix B: Computation of heat capacity in D -dimensional superconductors and superfluids

In this Appendix, we provide the calculation of the heat capacity considered in Sec. VII within the mean-field and Gaussian level with an extension to D -dimension. First of all, the contribution from the uniform superfluid order reads

$$\Delta C_0(T) = -\frac{T}{L^D} \frac{\partial^2 F_{s0}(T)}{\partial T^2}, \quad (\text{B1})$$

with $F_{s0}(T) = L^D [a(T)\psi_0^2 + b\psi_0^4/2]$ at the MF level. At the GF and the BKT level, F_{s0} is replaced with Eq. (21) and Eq. (53), respectively. Within the MF level, Eq. (11) yields

$$\Delta C_0^{(\text{MF})} = \begin{cases} 0 & (T \geq T_{c0}), \\ \frac{\alpha^2 k_B^2}{b} T & (T < T_{c0}). \end{cases} \quad (\text{B2})$$

By including the thermal fluctuations within the GF level, Eqs. (19) and (41) give

$$\Delta C_0^{(\text{GF})} = \begin{cases} 0 & (T \geq T_c), \\ \frac{\alpha^2 k_B^2}{b} A_- (2 - A_-) T & (T \lesssim T_c). \end{cases} \quad (\text{B3})$$

The contribution from the fluctuations given by Eq. (84) in the superfluid phase reads

$$\begin{aligned}\Delta C_{\text{fl}}^- &= -\frac{T}{L^D} \frac{\partial^2 F_{\text{fl}}^-(T)}{\partial T^2} \\ &= -\frac{k_B T}{L^D} \xi^2 \sum_{\mathbf{k}} \frac{\partial_T \xi^{-2} + T \partial_T^2 \xi^{-2}/2}{1 + \xi^2 k^2/2} \\ &+ \frac{k_B T^2}{2L^D} \xi^4 \sum_{\mathbf{k}} \left(\frac{\partial_T \xi^{-2}}{1 + \xi^2 k^2/2} \right)^2,\end{aligned}\quad (\text{B4})$$

where the coherence length

$$\xi(T)^2 = \begin{cases} \frac{2\gamma}{a(T) + 3b\psi_0^2} & (\text{MF}), \\ \frac{2\gamma}{a(T) + 2b\langle|\eta|^2\rangle + 3b(\psi_0^{(\text{GF})})^2} & (\text{GF}), \end{cases}\quad (\text{B5})$$

coincides with Eq. (76) in the superfluid phase. In the vicinity of criticality, Eq. (B5) yields the relations

$$|\xi(T \rightarrow T_{c0}^-)^2| = \frac{1}{2} |\xi(T \rightarrow T_{c0}^+)^2| \quad (\text{B6a})$$

$$|\partial_T \xi(T \rightarrow T_{c0}^-)^{-2}| = 2 |\partial_T \xi(T \rightarrow T_{c0}^+)^{-2}| \quad (\text{B6b})$$

within the MF level, and

$$|\xi(T \rightarrow T_c^-)^2| = \frac{A_-}{2A_+} |\xi(T \rightarrow T_c^+)^2| \quad (\text{B7a})$$

$$|\partial_T \xi(T \rightarrow T_c^-)^{-2}| = \frac{2A_-}{A_+} |\partial_T \xi(T \rightarrow T_c^+)^{-2}| \quad (\text{B7b})$$

by including the thermal fluctuations within the Gaussian level. Equation (B4) can be written as

$$\begin{aligned}\Delta C_{\text{fl}}^- &= -\frac{\Omega_D k_B T}{(2\pi)^D} \xi^{2-D} \left(\partial_T \xi^{-2} + \frac{T}{2} \partial_T^2 \xi^{-2} \right) \int_{\xi k_0}^{\xi \Lambda} dx \frac{x^{D-1}}{1 + x^2/2} \\ &+ \frac{\Omega_D k_B T^2}{2(2\pi)^D} \xi^{4-D} (\partial_T \xi^{-2})^2 \int_{\xi k_0}^{\xi \Lambda} dx \frac{x^{D-1}}{(1 + x^2/2)^2},\end{aligned}\quad (\text{B8})$$

where $\Omega_D = D\pi^{D/2}/\Gamma(D/2 + 1)$ is the volume of the D -dimensional unit sphere with $\Gamma(x)$ being the Gamma function. In the same manner, the heat capacity in the

normal phase is given by

$$\begin{aligned}\Delta C_{\text{fl}}^+ &= -\frac{T}{L^D} \frac{\partial^2 F_{\text{fl}}^+(T)}{\partial T^2} \\ &= -\frac{2k_B T}{L^D} \xi^2 \sum_{\mathbf{k}} \frac{\partial_T \xi^{-2} + T \partial_T^2 \xi^{-2}/2}{1 + \xi^2 k^2/2} \\ &+ \frac{k_B T^2}{L^D} \xi^4 \sum_{\mathbf{k}} \left(\frac{\partial_T \xi^{-2}}{1 + \xi^2 k^2/2} \right)^2 \\ &= -\frac{2\Omega_D k_B T}{(2\pi)^D} \xi^{2-D} \left(\partial_T \xi^{-2} + \frac{T}{2} \partial_T^2 \xi^{-2} \right) \int_{\xi k_0}^{\xi \Lambda} dx \frac{x^{D-1}}{1 + x^2/2} \\ &+ \frac{\Omega_D k_B T^2}{(2\pi)^D} \xi^{4-D} (\partial_T \xi^{-2})^2 \int_{\xi k_0}^{\xi \Lambda} dx \frac{x^{D-1}}{(1 + x^2/2)^2}.\end{aligned}\quad (\text{B9})$$

The most singular part is the second line in Eqs. (B8) and (B9) compared to each of the first terms, respectively. Using the relations (B6) and (B7), the singular part of the heat capacity in the vicinity of criticality provides the relation

$$\Delta C_{\text{fl}, \text{MF}}^- = 2^{D/2-1} \Delta C_{\text{fl}, \text{MF}}^+, \quad (\text{B10})$$

within the MF level [34], and

$$\Delta C_{\text{fl}, \text{GF}}^- = 2^{D/2-1} \left(\frac{A_-}{A_+} \right)^{4-D/2} \Delta C_{\text{fl}, \text{GF}}^+, \quad (\text{B11})$$

within the Gaussian level if $\xi \Lambda \rightarrow +\infty$ and $\xi k_0 \rightarrow 0$.

For $D = 2$, in particular, Eqs. (B10) and (B11) recover Eqs. (86) and (87), respectively. Practically, one obtains the overall heat capacity as

$$\begin{aligned}\Delta C^- &= \Delta C_0 + \Delta C_{\text{fl}}^- \\ &= \Delta C_0 - \frac{k_B T}{4\pi} \left(\partial_T \xi^{-2} + \frac{T}{2} \partial_T^2 \xi^{-2} \right) \ln \left(\frac{1 + \xi^2 \Lambda^2/2}{1 + \xi^2 k_0^2/2} \right) \\ &+ \frac{k_B T^2}{8\pi} \xi^2 (\partial_T \xi^{-2})^2 \left(\frac{1}{1 + \xi^2 k_0^2/2} - \frac{1}{1 + \xi^2 \Lambda^2/2} \right),\end{aligned}\quad (\text{B12a})$$

$$\begin{aligned}\Delta C^+ &= \Delta C_{\text{fl}}^+ \\ &= -\frac{k_B T}{2\pi} \left(\partial_T \xi^{-2} + \frac{T}{2} \partial_T^2 \xi^{-2} \right) \ln \left(\frac{1 + \xi^2 \Lambda^2/2}{1 + \xi^2 k_0^2/2} \right) \\ &+ \frac{k_B T^2}{4\pi} \xi^2 (\partial_T \xi^{-2})^2 \left(\frac{1}{1 + \xi^2 k_0^2/2} - \frac{1}{1 + \xi^2 \Lambda^2/2} \right).\end{aligned}\quad (\text{B12b})$$

The fluctuation contributions in Eqs. (B12) imply that a smaller infrared momentum cutoff k_0 enhances the heat capacity.

Appendix C: Heat capacity including vortex excitations in two-dimensional superconductors and superfluids

The heat capacity including the vortex excitations can be obtained as

$$\Delta C_{\text{BKT}} = \Delta C_0 + \Delta C_{\text{fl}}, \quad (\text{C1})$$

where ΔC_0 is given by Eq. (B1) with $D = 2$ under the substitution of $\psi_0 = \psi_R^{(BKT)}$ and $\Delta C_{\text{fl}} \equiv \Delta C_{\text{fl},\eta} + \Delta C_{\text{fl},\text{XY}}$

$$\begin{aligned}\Delta C_{\text{fl},\eta}^- &= -\frac{T}{L^2} \frac{\partial^2 F_{\text{fl}}^-}{\partial T^2} \\ &= -\frac{k_B T}{4\pi} \left(\partial_T \xi^{-2} + \frac{T}{2} \partial_T^2 \xi^{-2} \right) \ln \left(\frac{1 + \xi^2 \Lambda^2/2}{1 + \xi^2 k_0^2/2} \right) \\ &\quad + \frac{k_B T^2}{8\pi} \xi^2 (\partial_T \xi^{-2})^2 \left(\frac{1}{1 + \xi^2 k_0^2/2} - \frac{1}{1 + \xi^2 \Lambda^2/2} \right),\end{aligned}\quad (\text{C2})$$

and

$$\xi(T)^2 = \frac{2\gamma}{a(T) + 2b\langle|\eta|^2\rangle + \gamma\langle(\nabla\tilde{\theta})^2\rangle + 3b(\psi_R^{(BKT)})^2}. \quad (\text{C3})$$

Moreover, the XY free energy in Eq. (70) also contributes to the heat capacity as

$$\Delta C_{\text{fl},\text{XY}} = -\frac{T}{L^2} \frac{\partial^2 F_{\text{fl},\text{XY}}}{\partial T^2}. \quad (\text{C4})$$

-
- [1] V. L. Ginzburg and L. D. Landau, On the Theory of Superconductivity, *Zh. Eksp. Teor. Fiz.* **20**, 1064 (1950).
- [2] M. V. Milošević and R. Geurts, The Ginzburg-Landau theory in application, *Phys. C Supercond.* **470**, 791-795 (2010).
- [3] J. Carlström, E. Babaev, and M. Speight, Type-1.5 superconductivity in multiband systems: Effects of interband couplings, *Phys. Rev. B* **83**, 174509 (2011).
- [4] T. Kamatani, S. Kitamura, N. Tsuji, R. Shimano, and T. Morimoto, Optical response of the Leggett mode in multiband superconductors in the linear response regime, *Phys. Rev. B* **105**, 094520 (2022).
- [5] B. McNaughton, N. Pinto, A. Perali, and M. V. Milošević, Causes and Consequences of Ordering and Dynamic Phases of Confined Vortex Rows in Superconducting Nanostripes, *Nanomaterials* **12**, 4043 (2022).
- [6] S. A. Chen and K. T. Law, Ginzburg-Landau Theory of Flat-Band Superconductors with Quantum Metric, *Phys. Rev. Lett.* **132**, 026002 (2024).
- [7] J. M. Kosterlitz and D. J. Thouless, Ordering, metastability and phase transitions in two-dimensional systems, *J. Phys. C: Solid State Phys.* **6**, 1181 (1973).
- [8] D. R. Nelson and J. M. Kosterlitz, Universal Jump in the Superfluid Density of Two-Dimensional Superfluids, *Phys. Rev. Lett.* **39**, 1201 (1977).
- [9] D. J. Bishop and J. D. Reppy, Study of the Superfluid Transition in Two-Dimensional ^4He Films, *Phys. Rev. Lett.* **40**, 1727 (1978).
- [10] M. Mondal, S. Kumar, M. Chand, A. Kamlapure, G. Saraswat, G. Seibold, L. Benfatto, and P. Raychaudhuri, Role of the vortex-core energy on the Berezinskii-Kosterlitz-Thouless transition in thin films of NbN, *Phys. Rev. Lett.* **107**, 217003 (2011).
- [11] J. Yong, T. R. Lemberger, L. Benfatto, K. Ilin, and M. Siegel, Robustness of the Berezinskii-Kosterlitz-Thouless transition in ultrathin NbN films near the superconductor-insulator transition, *Phys. Rev. B* **87**, 184505 (2013).
- [12] Y. Nakagawa, Y. Kasahara, T. Nomoto, R. Arita, T. Nojima, and Y. Iwasa, Gate-controlled BCS-BEC crossover in a two-dimensional superconductor, *Science* **372**, 190-195 (2021).
- [13] A. Weitzel, L. Pfaffinger, I. Maccari, K. Kronfeldner, T. Huber, L. Fuchs, J. Mallord, S. Linzen, E. Il'ichev, N. Paradiso, and C. Strunk, Sharpness of the Berezinskii-Kosterlitz-Thouless Transition in Disordered NbN Films, *Phys. Rev. Lett.* **131**, 186002 (2023).
- [14] P. Christodoulou, M. Galka, N. Dogra, R. Lopes, J. Schmitt, and Z. Hadzibabic, Observation of first and second sound in a BKT superfluid, *Nature* **594**, 191 (2021).
- [15] K. Furutani, A. Tononi, and L. Salasnich, Sound modes in collisional superfluid Bose gases, *New J. Phys.* **23**, 043043 (2021).
- [16] L. Salasnich, A. Cappellaro, K. Furutani, A. Tononi, and G. Bighin, First and Second Sound in Two-Dimensional Bosonic and Fermionic Superfluids, *Symmetry* **14**, 2182 (2022).
- [17] Y. Wang, B. Revaz, A. Erb, and A. Junod, Direct observation and anisotropy of the contribution of gap nodes in the low-temperature specific heat of $\text{YBa}_2\text{Cu}_3\text{O}_7$, *Phys. Rev. B* **63**, 094508 (2001).
- [18] O. J. Taylor, A. Carrington, and J. A. Schlueter, Specific Heat Measurements of the Gap Structure of the Organic Superconductors $\kappa - (\text{ET})_2\text{Cu}[\text{N}(\text{CN})_2]\text{Br}$ and $\kappa - (\text{ET})_2\text{Cu}(\text{NCS})_2$, *Phys. Rev. Lett.* **99**, 057001 (2007).
- [19] T. D. Nguyen, A. Frydman, and O. Bourgeois, Investigation of specific heat in ultrathin two-dimensional superconducting Pb, *Phys. Rev. B* **101**, 014509 (2020).
- [20] Y. Mizukami, M. Haze, O. Tanaka, K. Matsuura, D. Sano, J. Böker, I. Eremin, S. Kasahara, Y. Matsuda, and T. Shibauchi, Unusual crossover from Bardeen-Cooper-Schrieffer to Bose-Einstein-condensate superconductivity in iron chalcogenides, *Commun. Phys.* **6**, 183 (2023).
- [21] C. A. R. Sá de Melo, M. Randeria, and J. R. Engelbrecht, Crossover from BCS to Bose superconductivity: Transition temperature and time-dependent Ginzburg-Landau

- theory, Phys. Rev. Lett. **71**, 3202 (1993).
- [22] N. D. Mermin and H. Wagner, Absence of Ferromagnetism or Antiferromagnetism in One- or Two-Dimensional Isotropic Heisenberg Models, Phys. Rev. Lett. **17**, 1133 (1966).
- [23] P. C. Hohenberg, Existence of Long-Range Order in One and Two Dimensions, Phys. Rev. **158**, 383 (1967).
- [24] A. Altland and B. Simons, *Condensed Matter Field Theory* (Cambridge University Press, Cambridge, 2010).
- [25] M. Franz and A. J. Millis, Phase fluctuations and spectral properties of underdoped cuprates, Phys. Rev. B **58**, 14572 (1998).
- [26] Y. Wang, L. Li, N. P. Ong, Nernst effect in high- T_c superconductors Phys. Rev. B **73**, 024510 (2006).
- [27] J. W. Loram, J. Luo, J. R. Cooper, W. Y. Liang, and J. L. Tallon, Evidence on the pseudogap and condensate from the electronic specific heat, J. Phys. Chem. Solids **62**, 59 (2001).
- [28] F. Marsiglio, P. Pieri, A. Perali, F. Palestini, and G. C. Strinati, Pairing effects in the normal phase of a two-dimensional Fermi gas, Phys. Rev. B **91**, 054509 (2015).
- [29] M. Feld, B. Fröhlich, E. Vogt, M. Koschorreck, and M. Köhl, Nature **480**, 75 (2011).
- [30] B. Fröhlich, M. Feld, E. Vogt, M. Koschorreck, M. Köhl, C. Berthod, and T. Giamarchi, Two-Dimensional Fermi Liquid with Attractive Interactions, Phys. Rev. Lett. **109**, 130403 (2012).
- [31] X. Wang, Q. Chen, and K. Levin, Strong pairing in two dimensions: pseudogaps, domes, and other implications, New J. Phys. **22**, 063050 (2020).
- [32] Z. Wang, G. Chaudhary, Q. Chen, and K. Levin, Quantum geometric contributions to the BKT transition: Beyond mean field theory, Phys. Rev. B **102**, 184504 (2020).
- [33] T. Shi, W. Zhang, and C. A. R. Sá de Melo, Tighter upper bounds on the critical temperature of two-dimensional superconductors and superfluids from the BCS to the Bose regime, arXiv:2303.10939.
- [34] A. Larkin and A. Varlamov, *Theory of Fluctuations in Superconductors* (Oxford University Press, Oxford, 2005).
- [35] J. Bardeen, L. N. Cooper, and J. R. Schrieffer, Microscopic Theory of Superconductivity, Phys. Rev. **106**, 162 (1957).
- [36] L. P. Gorkov, Microscopic Derivation of the Ginzburg-Landau Equations in the Theory of Superconductivity, Sov. Phys. JETP **36**, 1364 (1959).
- [37] A. Griffin, Conserving and gapless approximations for an inhomogeneous Bose gas at finite temperatures, Phys. Rev. B **53**, 9341 (1996); A. Griffin, T. Nikuni, and E. Zaremba, *Bose-Condensed Gases at Finite Temperatures* (Cambridge University Press, Cambridge, 2009).
- [38] G. Leibbrandt, Introduction to the technique of dimensional regularization, Rev. Mod. Phys. **74**, 849 (1975).
- [39] L. Salasnich, A. A. Shanenko, A. Vagov, J. Albino Aguiar, and A. Perali, Screening of pair fluctuations in superconductors with coupled shallow and deep bands: A route to higher-temperature superconductivity, Phys. Rev. B **100**, 064510 (2019).
- [40] A. Cappellaro and L. Salasnich, Shift of the critical temperature in superconductors: a self-consistent approach, Sci. Rep. **10**, 9088 (2020).
- [41] V. G. Kogan and J. Schmalian, Ginzburg-Landau theory of two-band superconductors: Absence of type-1.5 superconductivity, Phys. Rev. B **83**, 054515 (2011).
- [42] K. V. Grigorishin, Effective Ginzburg-Landau free energy functional for multi-band isotropic superconductors, Phys. Lett. A **380**, 1781 (2016).
- [43] H. T. C. Stoof, K. B. Gubbels, and D. B. M. Dickerscheid, *Ultracold Quantum Fields* (Springer, 2009).
- [44] P. Minnhagen and M. Nylen, Charge density of a vortex in the Coulomb-gas analogy of superconducting films, Phys. Rev. B **31**, 5768 (1985).
- [45] U. Al Khawaja, J. O. Andersen, N. P. Proukakis, and H. T. C. Stoof, Low dimensional Bose gases, Phys. Rev. A **66**, 013615 (2002).
- [46] W. Zhang, G.-D. Lin, and L.-M. Duan, Berezinskii-Kosterlitz-Thouless transition in a trapped quasi-two-dimensional Fermi gas near a Feshbach resonance, Phys. Rev. A **78**, 043617 (2008).
- [47] G. Bighin and L. Salasnich, Vortices and antivortices in two-dimensional ultracold Fermi gases, Sci. Rep. **7**, 45702 (2017).
- [48] G. Midei, K. Furutani, L. Salasnich, and A. Perali, Predictive power of the Berezinskii-Kosterlitz-Thouless theory based on Renormalization Group throughout the BCS-BEC crossover in 2D superconductors, arXiv:2403.03025.
- [49] J. F. Annett, *Superconductivity, Superfluids and Condensates* (Oxford University Press, 2003).
- [50] C. Timm, Theory of Superconductivity: Winter Semester 2011/2012 TU Dresden Institute of Theoretical Physics (2021).
- [51] M. Gräter and C. Wetterich, Kosterlitz-Thouless Phase Transition in the Two Dimensional Linear σ Model, Phys. Rev. Lett. **75**, 378 (1995).
- [52] G. v. Gersdorff and C. Wetterich, Nonperturbative renormalization flow and essential scaling for the Kosterlitz-Thouless transition, Phys. Rev. B **64**, 054513 (2001).
- [53] P. Jakubczyk, N. Dupuis, and B. Delamotte, Reexamination of the nonperturbative renormalization-group approach to the Kosterlitz-Thouless transition, Phys. Rev. E **90**, 062105 (2014).
- [54] P. Jakubczyk and W. Metzner, Longitudinal fluctuations in the Berezinskii-Kosterlitz-Thouless phase, Phys. Rev. B **95**, 085113 (2017).
- [55] J. Krieg and P. Kopietz, Dual lattice functional renormalization group for the Berezinskii-Kosterlitz-Thouless transition: Irrelevance of amplitude and out-of-plane fluctuations, Phys. Rev. E **96**, 042107 (2017).
- [56] N. Defenu, A. Trombettoni, I. Nándori, and T. Enss, Nonperturbative renormalization group treatment of amplitude fluctuations for $|\varphi|^4$ topological phase transitions, Phys. Rev. B **96**, 174505 (2017).
- [57] M. Kobayashi, M. Eto, and M. Nitta, Berezinskii-Kosterlitz-Thouless Transition of Two-Component Bose Mixtures with Intercomponent Josephson Coupling, Phys. Rev. Lett. **123**, 075303 (2019).
- [58] K. Furutani, A. Perali, and L. Salasnich, Berezinskii-Kosterlitz-Thouless phase transition with Rabi-coupled bosons, Phys. Rev. A **107**, L041302 (2023).
- [59] G. Midei and A. Perali, Sweeping across the BCS-BEC crossover, reentrant, and hidden quantum phase transitions in two-band superconductors by tuning the valence and conduction bands, Phys. Rev. B **107**, 184501 (2023).
- [60] G. Midei and A. Perali, Giant amplification of Berezinskii-Kosterlitz-Thouless transition temperature in superconducting systems characterized by cooperative interplay of small-gapped valence and conduction bands,

- Phys. Scr. **99**, 045216 (2024).
- [61] S. K. Paramasivam, S. P. Gangadharan, M. V. Milošević, and A. Perali, High-T_c Berezinskii-Kosterlitz-Thouless transition in 2D superconducting systems with coupled deep and quasi-flat electronic bands with van Hove singularities, arXiv:2312.09017, Phys. Rev. B (2024), in press.